

Characterisation of reactor spectra

René Reifarh, Sophia Florence Dellmann, Deniz Kurtulgil

August 24, 2023

Contents

1	Introduction	1
2	Approach	3
3	User friendly code	4
4	Application of code	6
4.1	Example: Regular activation at TRIGA reactor Mainz	6
4.2	Example: Cadmium-encapsulated activation at TRIGA reactor Mainz	10

1 Introduction

Fig. 1 shows the components of a typical reactor spectrum.

Since the (n,γ) cross section falls rapidly with increasing energy, only two components need to be considered for neutron (capture) activations:

- Thermal component with the corresponding time-integrated flux ϕ^{th}
- Epithermal component with the corresponding time-integrated flux ϕ^{epi}

With the ratio of produced to sample nuclei of a given isotope of mass A

$$R_A = \frac{N_{A+1}}{N_A} \tag{1}$$

the simplified 2-component assumption can be expressed as:

$$R_A = \sigma_A^{th} \phi^{th} + \sigma_A^{epi} \phi^{epi} \tag{2}$$

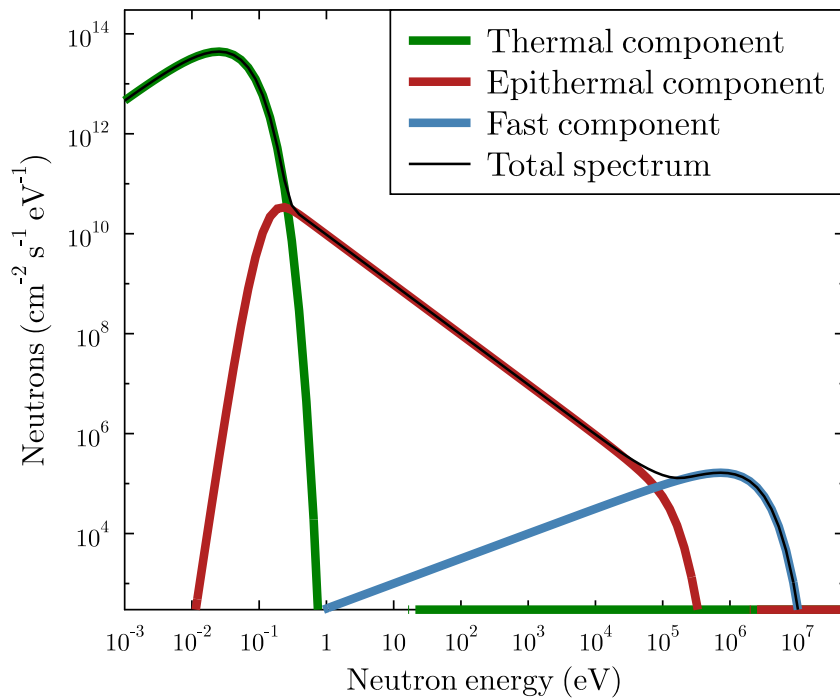


Figure 1: Components of a typical reactor neutron spectrum.

where σ_A^{th} is the thermal neutron capture cross section and σ_A^{epi} the resonance integral of isotope A .

2 Approach

The two components of the flux spectrum can only be disentangled if at least two monitors A and B with different ratios $\sigma_A^{epi}/\sigma_A^{th}$ and $\sigma_B^{epi}/\sigma_B^{th}$ are used. If only two monitor isotopes are used, the two corresponding equations (eq. (2)) result in a system of linear equations (SLE) and can be analytically solved for ϕ^{th} and ϕ^{epi} based on the experimentally determined production ratio $R_A^{exp} \pm dR_A^{exp}$ for each monitor, with the analytical solutions

$$\phi^{th} = \frac{\sigma_B^{epi} R_A - \sigma_A^{epi} R_B}{\sigma_B^{epi} \sigma_A^{th} - \sigma_A^{epi} \sigma_B^{th}} \quad (3)$$

$$\phi^{epi} = \frac{\sigma_A^{th} R_B - \sigma_B^{th} R_A}{\sigma_B^{epi} \sigma_A^{th} - \sigma_B^{th} \sigma_A^{epi}} \quad (4)$$

If more than 2 monitors are used, the SLE is overdetermined. The idea is now to determine the most likely pair of ϕ^{th} and ϕ^{epi} for the activation experiment. It is therefore necessary to construct the probability distribution for each flux pair and and each isotope. The following steps are necessary for each monitor:

1. Determine production ratio for each flux pair:

$$R_A^\phi = \sigma_A^{th} \phi^{th} + \sigma_A^{epi} \phi^{epi} \quad (5)$$

2. Determine uncertainty of production ratio for each flux pair based on the deviation from the experimentally determined production ratio and the combined uncertainties of the ratios:

$$dR_A^\phi = \sqrt{(\phi^{th} d\sigma_A^{th})^2 + (\phi^{epi} d\sigma_A^{epi})^2} \quad (6)$$

3. Determine probability distribution:

$$P_A^\phi = c_A \exp \left(-\frac{(R_A^\phi - R_A^{exp})^2}{2 \left((dR_A^\phi)^2 + (dR_A^{exp})^2 \right)} \right) \quad (7)$$

4. Determine the normalization constants c_A such that the integral is 1.

5. Combine the probability distributions for different isotopes with AND - hence the product:

$$P^\phi = c \prod c_A P_A^\phi \quad (8)$$

6. Determine the global normalization constant c such that the integral is 1.

3 User friendly code

The described approach is realized in a Fortran-90 based program and available at

```
exp-astro:/home/reifarh/nuetzliche_routinen/reactor_flux
```

Execution of the command

```
build_64bit_ubuntu_bash
```

will create an executable file named

```
analyze_flux
```

This step might be necessary, if the operating system changes or the approach itself needs to be changed. All experiment-specific information can (and should) be provided via simple ini-files. The command for execution might then be:

```
analyze_flux ta179_2021_regular.ini
```

The ini-file has a very simple structure (see Fig. 2) and examples for actual cases can be found in the same directory. It consists of

- 1 line determining the parameters for the x-axis (binning and range)
- 1 line determining the parameters for the y-axis (binning and range)
- 1 line determining the number of monitors used (no limitation)
- 3 lines per monitor containing (numbers simply space-separated)
 - name of monitor
 - 2 numbers: production ratio and uncertainty
 - 4 numbers: cross section and uncertainty for flux on x-axis, cross section and uncertainty for flux on y-axis (see 2D-plots in next chapter)

```

1  0. 1E16 300                                ! x-axis, min, ↵
   max, number of bins, e.g. thermal flux
2  0. 4E14 300                                ! y-axis, min, ↵
   max, number of bins, e.g. epithermal flux
3  3                                           ! number of ↵
   monitors
4  '94Zr'                                     ! name of monitor
5  2.77725958301662E-10  5.27141370494734E-12 ! ratio atoms ↵
   produced / sample for 1st monitor
6  4.98E-26  0.0017E-24  2.65E-25  0.01E-24 ! cross section ↵
   + uncert for flux on x-axis , cross section + uncert for flux ↵
   on y-axis
7  '96Zr'                                     ! name of monitor
8  1.26962284330168E-09  4.12183803591394E-11 ! ratio atoms ↵
   produced / sample for 2nd monitor
9  2.285E-26  0.001E-24  5.15E-24  0.11E-24 ! cross section ↵
   + uncert for flux on x-axis , cross section + uncert for flux ↵
   on y-axis
10 '197Au'                                    ! name of monitor
11 8.16E-07  3.09779867936006E-08            ! ratio atoms ↵
   produced / sample for 2nd monitor
12 9.867E-23  0.09E-24  1.55E-21  28E-24    ! cross section ↵
   + uncert for flux on x-axis , cross section + uncert for flux ↵
   on y-axis
13
14
15

```

- 1 -

Figure 2: Example of an actual ini-file. Please note the line numbers on the left and the symbols for line wraps on the right. The line wraps are only for the print-out. Everything past the exclamation marks is comment.

4 Application of code

If the program is executed, it reads the ini-file, calculates the probability distributions, determines the projections onto x- and y-axis and prints the mean and root-mean-square of the projections in the terminal.

In addition, some graphical output is provided / prepared. If gle is installed, actual graphic files in 'png' and 'pdf' format will be automatically created.

If the number of bins requested in x and y direction are identical and at most 1000, plots of 2D-histograms of the final probability distribution are produced during the graphical output (e.g. Figs. 3,6).

The graphical output always contains figures of x- and y-projections of the final probability distribution (e.g. Figs. 4,7) and plots with probability bands per monitor (e.g. Figs. 5, 9).

4.1 Example: Regular activation at TRIGA reactor Mainz

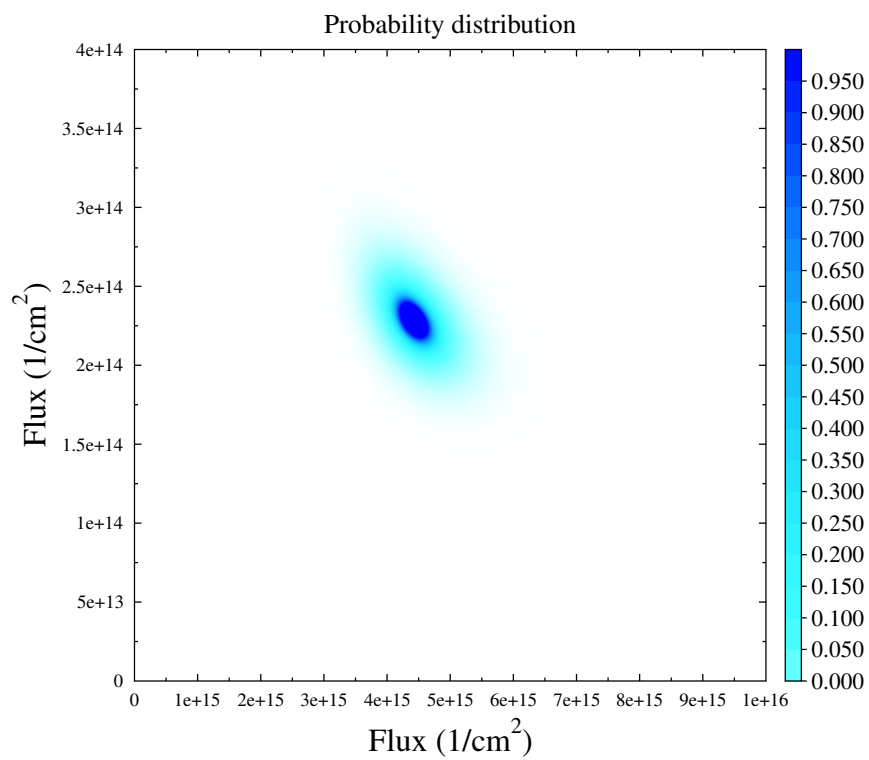


Figure 3: Regular activation, 3 monitors: ^{94,96}Zr and ¹⁹⁷Au. Probability distribution of the values for thermal flux (x-axis) and epithermal flux (y-axis).

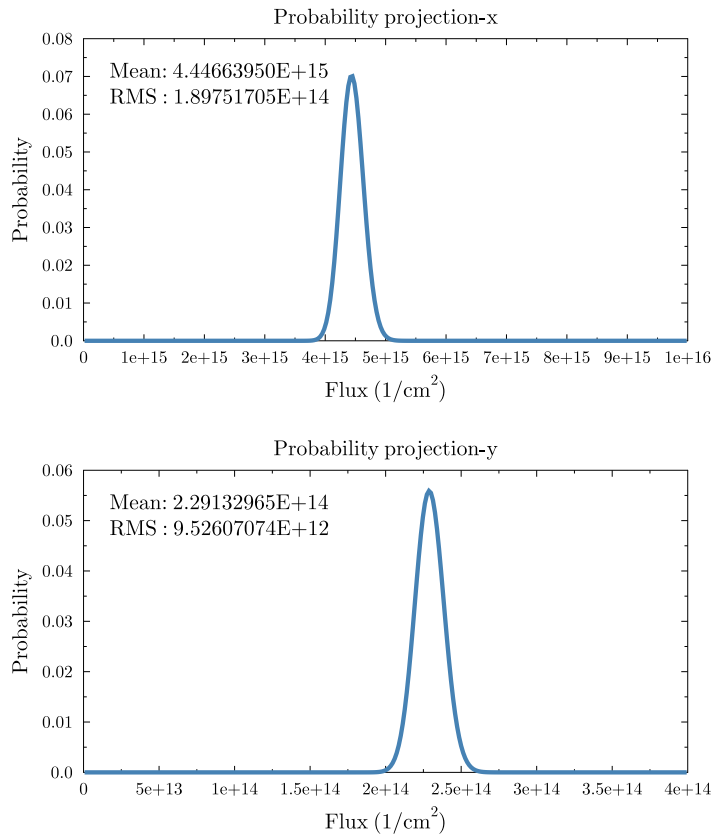


Figure 4: Regular activation, 3 monitors: $^{94,96}\text{Zr}$ and ^{197}Au . Projection of probability distribution (Fig. 3) onto x-axis (thermal flux) and y-axis (epithermal flux). Provided in the plot are the mean and root mean square of the respective distributions.

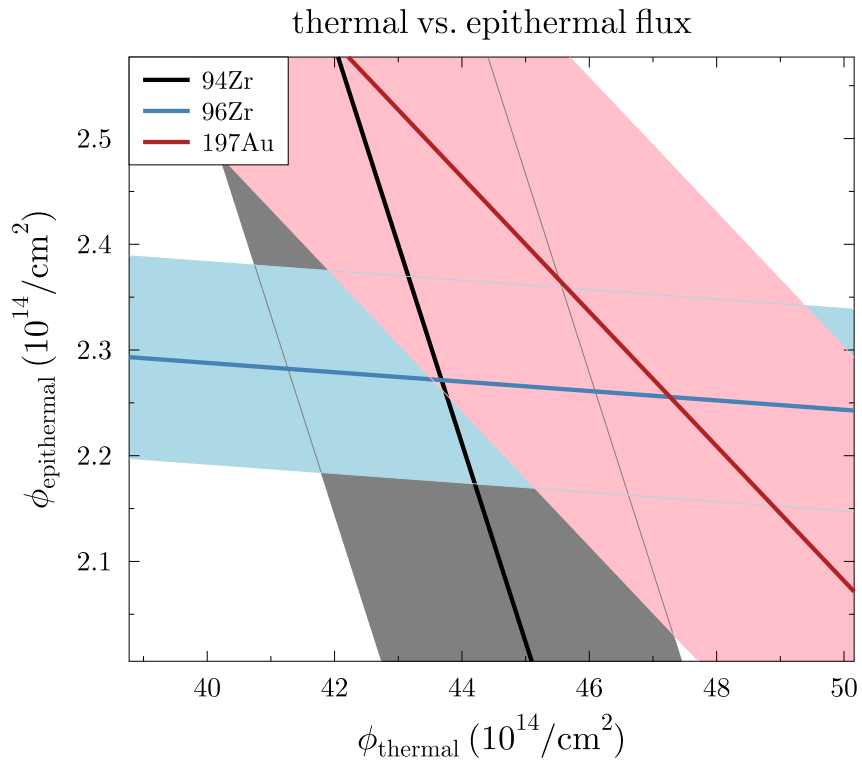


Figure 5: Regular activation, 3 monitors: $^{94,96}\text{Zr}$ and ^{197}Au . This plots illustrates the impact of additional monitors. Each single monitor give a line between 100% epithermal neutron flux (y-axis) and 100% thermal neutron flux (x-axis). The different ratios of thermal cross section an resonance intergral result in different lines for each monitor. Ideally, all line would intercept in one single point. The bands around each point represent the major part of the involved 1σ -uncertainties from the determined yield and cross sections. In a small region, all uncertainty bands incercept.

4.2 Example: Cadmium-encapsulated activation at TRIGA reactor Mainz

In particular in this run, the impact of additional monitors can be nicely observed, Fig 8. Relative to the thermal capture cross section, ^{45}Sc has the smallest resonance integral. It is therefore a very valuable addition to the other 3 monitors $^{94,96}\text{Zr}$ and ^{197}Au to constrain the very small thermal neutron flux inside the cadmium encapsulation.

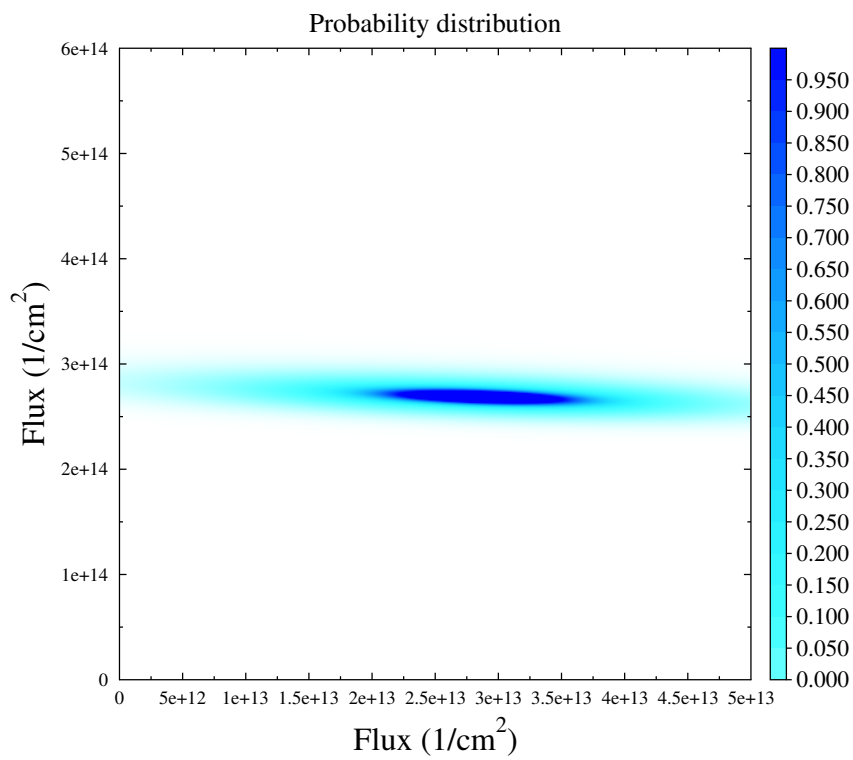


Figure 6: Activation with cadmium encapsulation, 4 monitors: ^{45}Sc , $^{94,96}\text{Zr}$ and ^{197}Au . Probability distribution of the values for thermal flux (x-axis) and epithermal flux (y-axis).

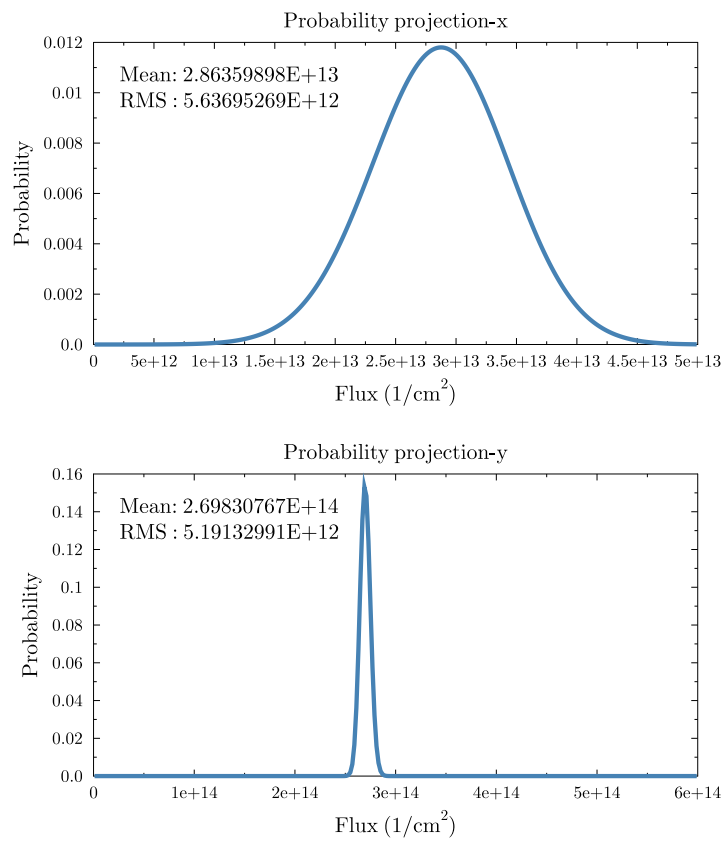


Figure 7: Activation with cadmium encapsulation, 4 monitors: ^{45}Sc , $^{94,96}\text{Zr}$ and ^{197}Au . Projection of probability distribution (Fig. 6) onto x-axis (thermal flux) and y-axis (epithermal flux). Provided in the plot are the mean and root mean square of the respective distributions.

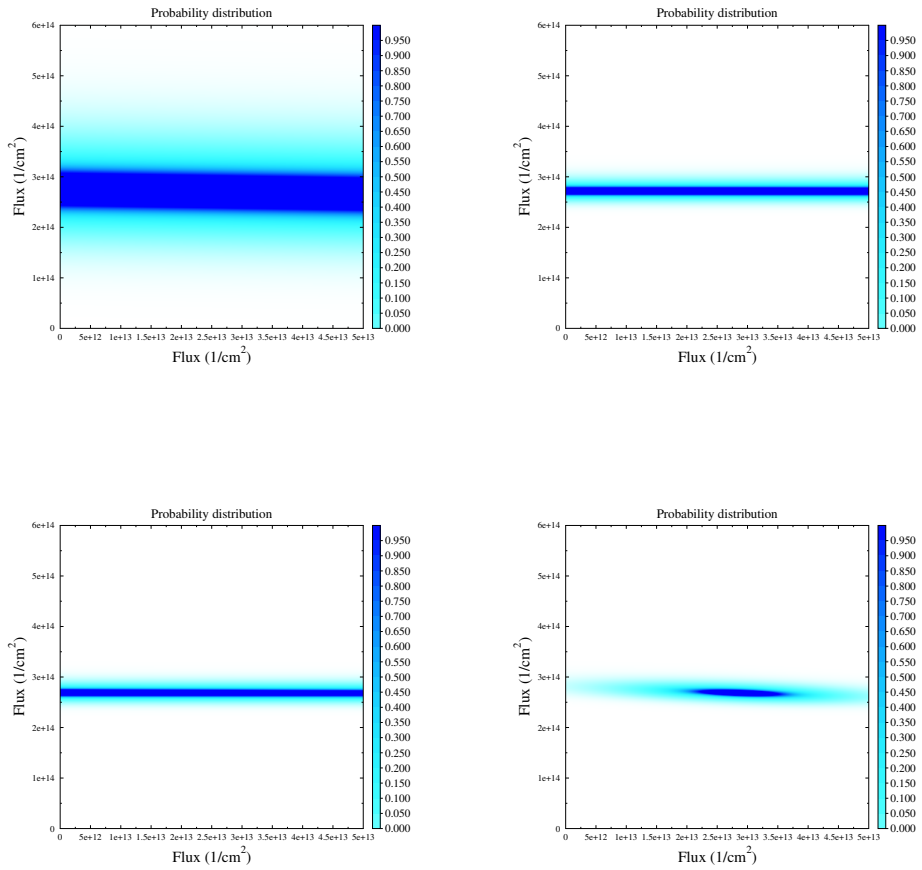


Figure 8: Activation with cadmium encapsulation. Probability distribution of the values for thermal flux (x-axis) and epithermal flux (y-axis).

Top left: 1 monitor: ^{94}Zr

Top right: 2 monitors: $^{94,96}\text{Zr}$

Bottom left: 3 monitors: $^{94,96}\text{Zr}$, ^{197}Au

Bottom right: 4 monitors: ^{45}Sc , $^{94,96}\text{Zr}$, ^{197}Au

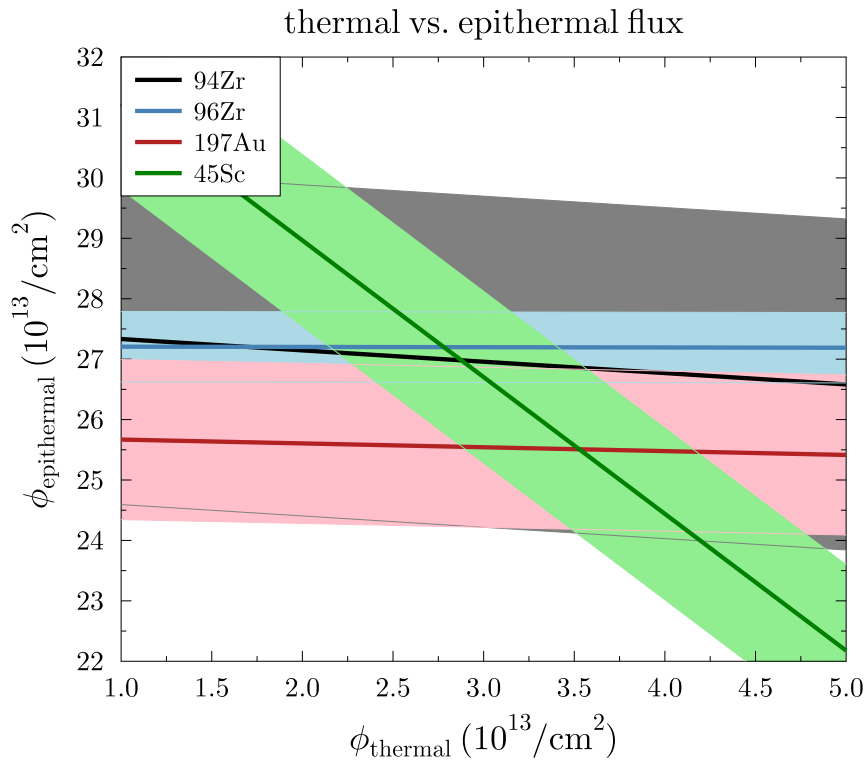


Figure 9: Activation with cadmium encapsulation, 4 monitors: ^{45}Sc , $^{94,96}\text{Zr}$ and ^{197}Au . This plots illustrates the impact of additional monitors. Each single monitor give a line between 100% epithermal neutron flux (y-axis) and 100% thermal neutron flux (x-axis). The different ratios of thermal cross section an resonance intergral result in different lines for each monitor. Ideally, all line would intercept in one single point. The bands around each point represent the major part of the involved 1σ -uncertainties from the determined yield and cross sections. In a small region, all uncertainty bands incercept.